ACS OMEGA

Open Access

http://pubs.acs.org/journal/acsodf

Article

Engineering Temperature-Responsive Polymer Nanoparticles that Load and Release Paclitaxel, a Low-Molecular-Weight Anticancer Drug

Hiroyuki Koide,* Kazuma Yamaguchi, Keijiro Sato, Maki Aoshima, Shoko Kanata, Sei Yonezawa, and Tomohiro Asai

Cite This: *ACS Omega* 2024, 9, 1011−1019

Read Online

ACCESS | Metrics & More | Article Recommendations | Supporting Information

ABSTRACT: Poly(*N*-isopropylacrylamide) (pNIPAm) undergoes a hydrophilicity/hydrophobicity change around its lower critical solution temperature (LCST). Therefore, pNIPAm-based polymer nanoparticles (NPs) shrink above their LCST and swell below their LCST. Although temperature responsiveness is an important characteristic of synthetic polymers in drug and gene delivery, few studies have investigated the temperature-responsive catch and release of low-molecular-weight drugs (LMWDs) as their affinity to the target changes. Since LMWDs have only a few functional groups, preparation of NPs with high affinity for LMWDs is hard compared with that for peptides and proteins. However, LMWDs such as anticancer drugs often have a stronger effect than peptides and proteins. Therefore, the development of NPs that can load and release LMWDs is needed for drug delivery. Here, we engineered pNIPAm-based NPs that capture paclitaxel (PTX), an anticancer LMWD that inhibits microtubules, above their LCST and release it below their LCST. The swelling transition of the NPs depended on their hydrophobic monomer structure. NPs with swelling ratios (=NP size at 25 °C/NP size at 37 °C) exceeding 1.90 released captured PTX when cooled to below their LCST by changing the affinity for PTX. On the other hand, NPs with a swelling ratio of only 1.14 released melittin. Therefore, optimizing the functional monomers of temperature-responsive NPs is essential for the catch and release of the target in a temperature-dependent manner. These results can guide the design of stimuli-responsive polymers that catch and release their target molecules.

INTRODUCTION

Protein−protein interactions are a nexus of multiple noncovalent interactions such as electrostatic and hydrophobic interactions and hydrogen bonds. Synthetic polymers such as linear polymers,[1] dendrimers,[2] and nanoparticles (NPs)[3] bind to their target molecules by incorporating functional groups that induce noncovalent interactions to their target. Functionalized synthetic polymers are used in small molecule,[4] nucleic acid,[4] and protein[5] capture, tissue engineering,[6] and disease therapy.[7] Such synthetic polymers have attracted interest as cost-effective abiotic affinity reagents. Interestingly, the characteristics of several synthetic polymers respond to their physical environment.[8] For instance, the hydrophilicity/hydrophobicity, charge, and volume of a polymer can change with pH,[9] light,[10] temperature,[11] and electric field.[12] These stimuli-responsive polymers are potentially useful for diagnostic applications and disease therapy.[13]

Poly(*N*-isopropylacrylamide) (pNIPAm)-based polymers are known as stimuli-responsive polymers[14] that reversibly change their hydrophilicity/hydrophobicity around their lower critical solution temperature (LCST, ∼ 32 °C).[15] Below the LCST, pNIPAm-based polymers are hydrophilic and interact with water molecules, but above the LCST, they are hydrophobic and undergo pNIPAm−pNIPAm interactions.[16] Consequently, pNIPAm exhibits a coil-to-globule transition at temperatures above its LCST. Lightly cross-linked pNIPAm-based polymer NPs extract water molecules and swell below their LCST; conversely, they exclude water molecules and shrink above their LCST.[17] This hydrophilicity/hydrophobicity change alters the affinity of NPs to their target.[18,19] The affinity change around the LCST has been exploited in protein purification[17] and switchable on/off catalytic reagents.[20] The temperature-responsive characteristics of pNIPAm have attracted special attention in drug discovery because the LCST of pNIPAm can be rigorously controlled by optimizing the structure and composition of the functional monomer.[21]

Low-molecular-weight drugs (LMWDs) such as paclitaxel (PTX) and doxorubicin can be physically loaded into the swollen polymer matrix of NPs above their LCST and squeezed from the NPs by heating above their LCST. The swollen polymer NPs collapse after heating or a pH decrease.[22] Although the squeezing-out strategy shows a considerable anticancer effect in vivo, loaded LMWDs will slowly leak from the polymers unless the temperature changes. Because the LMWDs packed into the swollen polymer network do not bind to the NPs, they passively diffuse, inducing side effects.[18,23] Previously, we developed NPs with a high affinity for melittin, a cytotoxic bee venom-derived peptide, above their LCST (37

Received: September 20, 2023
Revised: December 11, 2023
Accepted: December 13, 2023
Published: December 27, 2023

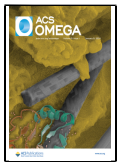

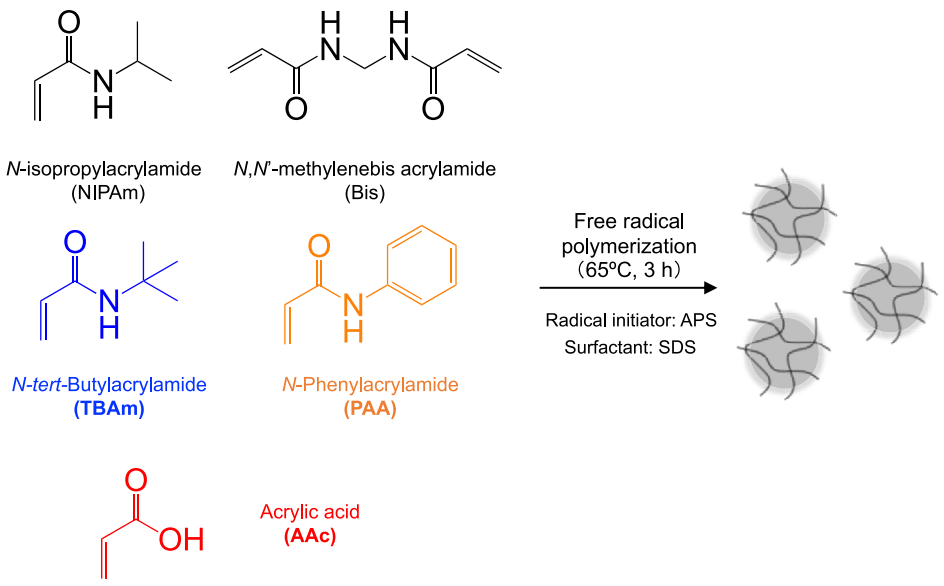

Figure 1. Synthesis of polymer NPs for PTX capture. Functional monomers used in NP synthesis for PTX capture and a schematic of NP synthesis.

Table 1. Monomer Compositions and the Sizes, Polydispersity Indices (PDIs), Swelling Ratio, and Yield of NPs at 25 and 37 °C[a]

	NIPAm	TBAm	PAA	bis	37°C		25°C		swelling ratio	yield (%)
					size (d nm)	PDI	size (d nm)	PDI		
control-NP	98			2	142 ± 12	0.005 ± 0.003	328 ± 18	0.007 ± 0.003	2.31 ± 0.09	80 ± 7
T1-NP	97	1		2	148 ± 8	0.006 ± 0.003	336 ± 27	0.007 ± 0.003	2.28 ± 0.08	72 ± 1
T3-NP	95	3		2	144 ± 3	0.006 ± 0.003	323 ± 7	0.006 ± 0.003	2.24 ± 0.07	68 ± 4
T5-NP	93	5		2	130 ± 8	0.005 ± 0.002	284 ± 17	0.008 ± 0.004	2.18 ± 0.04	69 ± 6
T10-NP	88	10		2	121 ± 4	0.003 ± 0.003	230 ± 15	0.006 ± 0.004	1.90 ± 0.07	73 ± 3
T20-NP	78	20		2	103 ± 2	0.006 ± 0.002	112 ± 4	0.006 ± 0.003	1.08 ± 0.06	77 ± 3
P1-NP	97		1	2	124 ± 1	0.005 ± 0.002	260 ± 1	0.007 ± 0.003	2.10 ± 0.01	80 ± 6
P3-NP	95		3	2	108 ± 7	0.007 ± 0.002	218 ± 162	0.006 ± 0.003	2.02 ± 0.08	90 ± 7
P5-NP	93		5	2	97 ± 7	0.006 ± 0.001	176 ± 12	0.008 ± 0.004	1.83 ± 0.03	82 ± 5
P10-NP	88		10	2	94 ± 16	0.004 ± 0.004	157 ± 28	0.006 ± 0.004	1.66 ± 0.05	85 ± 3
P20-NP	78		20	2	79 ± 1	0.007 ± 0.001	116 ± 11	0.006 ± 0.003	1.46 ± 0.02	81 ± 3

[a]Data represent the means ± standard errors (SEs). Swelling ratio = (NP size at 25 °C)/(NP size at 37 °C).

°C). After cooling to below their LCST (25 °C), this affinity is lost, and the NPs release the peptide for in vivo cancer therapy.[24] Intravenously injected melittin-captured NPs specifically released their melittin at the cooled tumor, inhibiting tumor growth in vivo without any side effects. This temperature-responsive affinity change strategy using pNIPAm-based NPs promises to be a unique drug-delivery method. However, pNIPAm-based NPs that catch and release LMWDs by changing their affinity at different temperatures have rarely been reported. In general, LMWDs such as anticancer drugs have a higher effect than peptides and proteins. Therefore, development of NPs that load and relase LMWDs is important to obtain the maximum effect and minimum side-effects. However, capturing a large amount of LMWDs by NPs and releasing it is difficult compared with that for peptides. Although NPs can create multipoint interactions with the melittin because melittin has many functional amino acids, they cannot create multipoint and multivalent interactions against LMWDs because of only a few functional groups in its molecules. Too much inclusion of the hydrophobic monomer decreases the LCST of NPs below 25 °C and will make it difficult to release LMWDs in response to temperature. Therefore, NPs that load and release LMWDs in response to temperature are a significant challenge.

In the present report, we engineered pNIPAm-based polymer NPs that capture PTX, an anticancer LMWD that inhibits microtubules (MW: 854), above the LCST (37 °C) and release it by cooling to below the LCST (25 °C). This strategy exploits the temperature-induced change in the affinity for PTX. When cooled to below their LCST, the NPs are hydrophilic and extract water molecules, causing swelling. As the swelling degree of the NPs indicates the degree of the hydrophobic-to-hydrophilic transition, we related the swelling degree of the NPs to the release of their captured PTX. The NPs bind to PTX (a highly hydrophobic small molecule) mainly via a hydrophobic interaction. Alternatively, we previously reported that pNIPAm-based NPs can be engineered to bind to the melittin peptide (a middle-molecular-weight peptide, MW: 2847). The engineered NPs bind to the melittin peptide by combining electrostatic and hydrophobic interactions.[25] We hypothesized that these different binding modes affect the swelling degree required to release the captured target molecules. Therefore, we also compared the required NP swelling degrees for releasing the

https://doi.org/10.1021/acsomega.3c07226
ACS Omega 2024, 9, 1011−1019

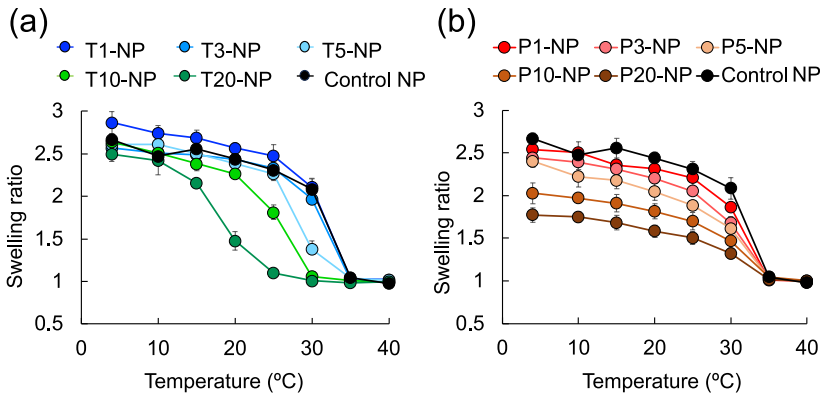

Figure 2. Swelling transitions of TBAm and PAA NPs. Measured sizes of (a) TBAm NPs and (b) PAA NPs and calculated swelling ratios (measured size/size at 37 °C) at 4, 15, 20, 25, 30, 35, and 40 °C (n = 3).

PTX and peptide. We demonstrated that the PTX capture and release amount depends on the hydrophobic monomer structure and percentage in NPs. After optimizing the functional monomer structure and percentage in NPs, the NPs captured PTX with a high affinity at 37 °C and easily released it when cooled to 25 °C. The NPs required a higher swelling degree for PTX release than for melittin release. Although temperature-responsive polymers have been widely reported, we report the first demonstration of the catch and release of LMWDs through temperature-responsive affinity changes. We also report the relationship between the swelling degree of NPs and LMWDs and the peptide release. The present study provides fundamental information for preparing temperature-responsive polymers for biomedical applications.

RESULTS AND DISCUSSION

Preparation of NPs with Affinity to PTX. Our goal is to develop NPs that catch and release PTX in a temperature-dependent manner. Previously, we reported that the normal temperature of the mouse body (~35 °C) decreases to 20 °C after cooling the mouse skin with ice.[24] Therefore, we engineered NPs that capture and release PTX at 37 and 25 °C, respectively. As PTX is a hydrophobic aromatic compound, we formed hydrophobic and/or $\pi-\pi$ stacking interactions of a hydrophobic monomer [*N*-*tert*-butylacrylamide (TBAm) or *N*-phenylacrylamide (PAA)] against PTX. NIPAm-based NPs were prepared via modified precipitation polymerization[26] of a functional monomer [NIPAm, *N*,*N*′-methylenebis(acrylamide) (bis)] and a hydrophobic monomer (TBAm or PAA) followed by dialysis purification (Figure 1). Given that a pNIPAm-based polymer with a large amount of the hydrophobic monomer loses its temperature-responsive property between 25 and 37 °C,[27] we maintained a low percentage of the hydrophobic monomer (0−20 mol %) in our prepared NPs. Table 1 summarizes the monomer composition of the NPs, their sizes at 37 and 25 °C, and their swelling ratios (25 °C/37 °C size ratio). The NP size was constant (~150 nm) at 37 °C but depended on the percentage of the hydrophobic monomer at 25 °C. The control NPs (without the hydrophobic monomer) were sized ~300 nm at 25 °C, and their swelling ratio was 2.31. In the experimental NPs, the swelling ratio initially showed no significant change and thereafter decreased as the TBAm percentage increased beyond 5 mol %. The temperature-dependent change in the particle size was lost when the TBAm percentage reached 20%. The PAA NP samples P1-NP and P3-NP exhibited slightly smaller swelling ratios (2.10 and 2.02, respectively) than the control NP (swelling ratio = 2.31). The swelling ratio of P20-NP was 1.46. Previous studies reported a similar decrease in the swelling ratio with increasing percentage of the hydrophobic monomer.[24,28,29] However, the temperature-responsive particle swelling tended to be more sensitive to the PAA content than to the TBA content, as evidenced by the higher swelling ratio of P20-NP (1.46) to T20-NP (1.08). Therefore, the temperature response of particle swelling depends on the structure of the hydrophobic monomer in the pNIPAm-based NPs. NMR data of NPs are shown in the Supporting Information figures.

Next, we measured the transition patterns of the NP swelling ratio as the temperature increased from 4 to 40 °C (size at each temperature/size at 37 °C). The size of the control NPs began increasing at 35 °C. The sizes of the TBAm NP samples (T1-, T3-, and T5-NP) also began increasing at 35 °C (Figure 2a), but the onset temperature of particle size increase decreased to 30 °C in T10-NP and 25 °C in T20-NP. These results indicate that increasing TBAm percentage decreases the onset temperature of particle size increase. The maximum swelling ratios of the TBAm NPs were ~2.5 regardless of TBAm percentage. The swelling ratio trends of the PAA NPs differed from those of the TBAm NPs (Figure 2b). Although the onset temperature of the particle size increase remained at 35 °C, the swelling ratio decreased with increasing PAA percentage. These results indicated that the TBAm percentage does not change the swelling ratio but changes the onset temperature of the particle size increase. In contrast, the PAA percentage does not change the onset temperature of the particle size increase but changes the swelling ratio. The onset temperature of the NP size increase is known to depend on the percentage of the hydrophobic monomer.[28,29] In addition, increasing the amount of the TBAm or PAA monomer reportedly decreases the onset temperature of NP size increase,[28,30] contradicting our present results on PAA NPs. These results indicate that the swelling pattern of pNIPAm NPs is dependent on the hydrophobic monomer structure.

Temperature-Responsive Catch and Release of PTX by NPs. To evaluate the influence of NP swelling on PTX release, we demonstrated the PTX capture and release ability of the NPs at 37 and 25 °C (Figure 3a). [^{3}H]-labeled PTX (100 nM) and NPs (1 mg/mL) were incubated at 37 or 25 °C for 30 min, and the PTX capture amount at each temperature was determined from the radioactivity measurements after ultracentrifugation. The PTX capture amount by the NPs

https://doi.org/10.1021/acsomega.3c07226
ACS Omega 2024, 9, 1011−1019

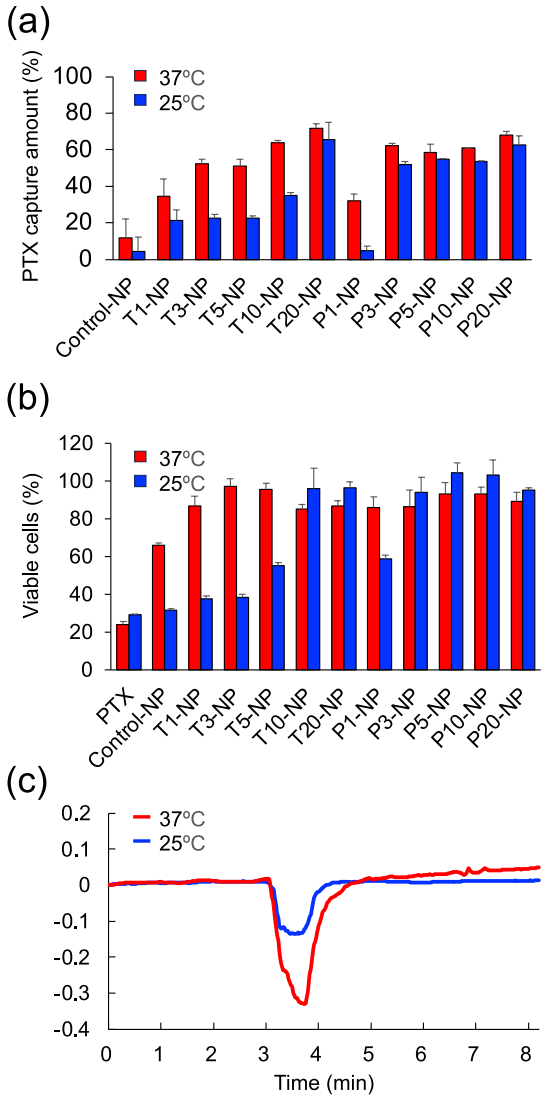

Figure 3. Temperature-responsive catch and release of PTX by the NPs. (a) NPs (1.0 mg/mL) and ^{3}H-PTX (100 nM) were incubated for 30 min at 37 °C. To measure the PTX release amount from NPs, incubation was continued for 30 min at 25 °C. After ultracentrifugation, the radioactivity of ^{3}H-PTX in the supernatant was measured. (b) NPs (1.0 mg/mL) and PTX (100 nM) were incubated for 30 min at 37 °C and additionally incubated for 30 min at 25 °C. After ultracentrifugation, the C26 NL-17 cells were incubated with the supernatant for 72 h at 37 °C, and the viable cells were measured by the WST-8 assay. (c) PTX was injected into T5-NP solution. Raw heat profiles were determined via a MicroCal PEAQ-ITC analysis.

depended on the percentage of the hydrophobic monomer in the NPs. More specifically, T1 and P1-NP (with 1% hydrophobic monomer) captured ∼40% of the PTX. After increasing the hydrophobic monomer percentage to 20%, more than 70% of the PTX was captured at 37 °C, indicating that a large amount of the hydrophobic monomer is important for capturing a large amount of PTX. The PTX capture amounts of T1, T3, T5, T10, and P1-NP were significantly lower at 25 °C than at 37 °C, but those of T20-, P3-, P5-, P10-, and P20-NP did not differ between the two temperatures. The drug loading capacity of NPs at 37 and 25 °C was shown in Table 2. Next, the anticancer effect of the released PTX was tested in vitro (Figure 3b). For this purpose, PTX (100 nM) and NPs (1 mg/mL) were incubated at 37 °C for 30 min. The PTX and

Table 2. Drug Loading Capacity of NPs at 37 and 25 °C[a]

	drug loading capacity (ng/1 mg NPs)	
	37°C	25°C
control-NP	10 ± 9	6 ± 4
T1-NP	30 ± 8	18 ± 5
T3-NP	45 ± 2	19 ± 2
T5-NP	44 ± 3	19 ± 2
T10-NP	55 ± 1	30 ± 1
T20-NP	61 ± 2	61 ± 2
P1-NP	27 ± 3	4 ± 2
P3-NP	53 ± 1	44 ± 2
P5-NP	50 ± 4	47 ± 1
P10-NP	52 ± 1	45 ± 1
P20-NP	58 ± 2	53 ± 2

[a]Data represent the means ± SEs. Drug loading capacity = (PTX ng)/(1 mg NPs).

NPs complex was then incubated at 25 °C for 30 min, and the PTX bound to NPs was removed through ultracentrifugation. The supernatant was added to murine colon cancer (C26-NL17) cells. After 24 h of incubation, the viable cells were determined by the WST-8 assay. The cell viability was correlated with the PTX capture amount at 25 and 37 °C. In the cultures incubated with the supernatant after PTX and NPs incubation at 37 °C, the cell viability exceeded 85%, indicating that all NPs (except the control NPs) inhibited almost all PTX release at 37 °C. When the supernatant was added after the PTX and T10-, T20-, P3-, P5-, P10-, or P20-NP incubation, cell viabilities did not change substantially between 37 and 25 °C. In contrast, cell viabilities by adding the supernatant after PTX and T1-, T3-, T5-, T10-, or P1-NP incubation were remarkably lower at 25 °C than at 37 °C. Focusing on the swelling ratio of the NPs, the PTX releases from the TBAm and PAA NPs with swelling ratios exceeding 1.90 and 2.10, respectively. Therefore, we concluded that a large change in the particle size is required for the release of hydrophobic small molecules, such as PTX from temperature-responsive pNIPAm-based NPs.

The PTX capture amounts in the NPs differed at 37 and 25 °C. To confirm that the temperature-dependent PTX capture amount arises from the altered affinity of NPs to PTX, we measured the interaction between T5-NP and PTX at 37 and 25 °C using isothermal titration calorimetry (ITC). PTX was injected once into a cell culture containing T5-NP dissolved in 5 mM phosphate buffer (pH 7.4), and the thermal change was monitored (Figure 3c). The ΔQ (heat change) after injecting PTX was 2.7 μcal at 25 °C and 13.2 μcal at 37 °C. This result indicates that T5-NP released its captured PTX because its affinity for PTX at 37 °C was lost at 25 °C.

Temperature-Responsive Size Change of the AAc-Containing NPs. The NPs required a large swelling ratio to elicit temperature-responsive PTX release. As PTX is a hydrophobic aromatic molecule, it should be captured by the NPs via hydrophobic (single-valent) interactions. Previously, we reported that NPs prepared with AAc (a negatively charged monomer) and TBAm capture melittin, a middle-molecular-weight-peptide (MW: 2847), at 37 °C and release it at 25 °C.[24] The NPs bind to melittin via combined electrostatic and hydrophobic (multivalent) interactions. Given the different binding characteristics of NP−PTX and NP−melittin (single-valent versus multivalent), we hypothesized that the required swelling degree of the NPs differs between PTX and melittin

https://doi.org/10.1021/acsomega.3c07226
ACS Omega 2024, 9, 1011−1019

Table 3. Monomer Compositions and the Sizes, PDIs, and Swelling Ratios of the NPs at 25 and 37 °C[a]

	NIPAm	TBAm	PAA	AAc	bis	37°C		25°C		swelling ratio
						size (d nm)	PDI	size (d nm)	PDI	
T5-A5-NP	88	5		5	2	163 ± 25	0.096 ± 0.0017	609 ± 89	0.021 ± 0.018	3.75 ± 0.21
T10-A5-NP	83	10		5	2	151 ± 25	0.061 ± 0.046	433 ± 45	0.107 ± 0.095	2.89 ± 0.20
T15-A5-NP	78	15		5	2	136 ± 24	0.058 ± 0.015	214 ± 42	0.117 ± 0.086	1.57 ± 0.19
T20-A5-NP	73	20		5	2	131 ± 15	0.073 ± 0.042	149 ± 14	0.054 ± 0.068	1.14 ± 0.04
T25-A5-NP	68	25		5	2	120 ± 17	0.050 ± 0.042	131 ± 25	0.051 ± 0.034	1.09 ± 0.11
T30-A5-NP	63	30		5	2	107 ± 17	0.081 ± 0.045	111 ± 13	0.078 ± 0.011	1.04 ± 0.03
P5-A5-NP	88		5	5	2	111 ± 15	0.031 ± 0.022	270 ± 52	0.081 ± 0.131	2.43 ± 0.18
P10-A5-NP	83		10	5	2	94 ± 10	0.059 ± 0.019	193 ± 36	0.129 ± 0.054	2.04 ± 0.17
P15-A5-NP	78		15	5	2	90 ± 3	0.105 ± 0.048	173 ± 13	0.038 ± 0.023	1.91 ± 0.07
P20-A5-NP	73		20	5	2	89 ± 3	0.073 ± 0.007	157 ± 11	0.070 ± 0.022	1.76 ± 0.06
P25-A5-NP	68		25	5	2	87 ± 2	0.083 ± 0.048	140 ± 11	0.083 ± 0.028	1.61 ± 0.08
P30-A5-NP	63		30	5	2	86 ± 4	0.085 ± 0.007	128 ± 13	0.075 ± 0.064	1.47 ± 0.09

[a]Data represent the means ± SEs.

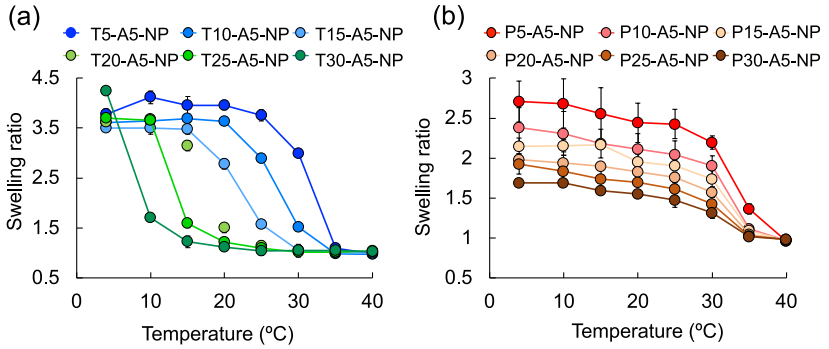

Figure 4. Swelling transitions of AAc-containing NPs: measured sizes of (a) TBAm−AAc−NPs and (b) PAA−AAc−NPs and calculated swelling ratios (measured size/size at 37 °C) at 4, 15, 20, 25, 30, 35, and 40 °C (n = 3).

release. To demonstrate this hypothesis, we prepared NPs with NIPAm, Bis (2 mol %), and AAc (5 mol %) along with TBAm (5−30 mol %) or PAA (5−30 mol %) for melittin capture. The NPs were generated through modified precipitation polymerization (Figure 1). The monomer compositions, sizes at 37 and 25 °C, and swelling ratios of the prepared NPs are listed in Table 3. The NP sizes were approximately 80−150 nm at 37 °C and 100−500 nm at 25 °C. The swelling ratio depended on the percentage of the hydrophobic monomer in the polymer. The swelling ratios of the TBAm and PAA NPs were 1.04 and 1.47−2.43, respectively. The swelling ratio was slightly higher in NPs containing the anionic monomer (AAc) than in non-AAc NPs, probably because AAc induces electric repulsion in the NPs.

We next measured the temperature dependence of the swelling ratio in the AAc-incorporated NPs (Figure 4). Here, the temperature was ranged from 4 to 40 °C. The transition patterns of the NP swelling ratio were similar in the NPs with and without AAc. Meanwhile, increasing the TBAm percentage in the TBAm NPs decreased the onset temperature of NP size increase but little affected the swelling ratio, which hovered around 3.5−4.0. In contrast, increasing the PAA percentage hardly affected the onset temperature of the size increase in the PAA NPs but decreased the swelling ratio. According to these results, a small amount of AAc (5%) in the NPs does not change the NP swelling trends.

Temperature-Responsive Catch and Release of Melittin by the AAc-Containing NPs. The temperature-responsive relationship between the swelling ratio and melittin release from the NPs was investigated through a hemolysis assay (Figure 5). Red blood cells (RBCs) were incubated with

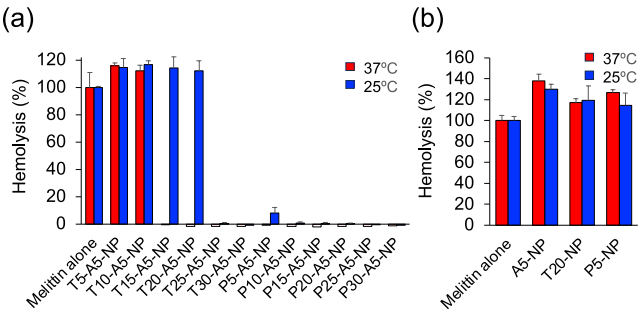

Figure 5. Temperature-respondent catch and release of melittin by NPs: red blood cells were incubated with NPs (0.3 mg/mL) and melittin (6 μM) for 120 min at 37 or 25 °C. The hemolysis ratio was determined from the measured absorbance of hemoglobin (405 nm).

NPs (1 mg/mL) and melittin (6×10^{-6} M) for 120 min at 37 or 25 °C. The hemolysis percentage was determined from the hemoglobin absorbance (405 nm) after centrifugation (10,000g for 10 min at 4 °C). Hemolysis was not inhibited by T5-A5-NP and T10-A5-NP at 37 or 25 °C but was inhibited by T25-A5-NP and T30-A5-NP at both temperatures, indicating that T5-A5-NP and T10-A5-NP captured no melittin at these temperatures and released no melittin upon cooling. We previously reported that both electrostatic and hydrophobic interactions are required for melittin capture by

https://doi.org/10.1021/acsomega.3c07226
ACS Omega 2024, 9, 1011−1019

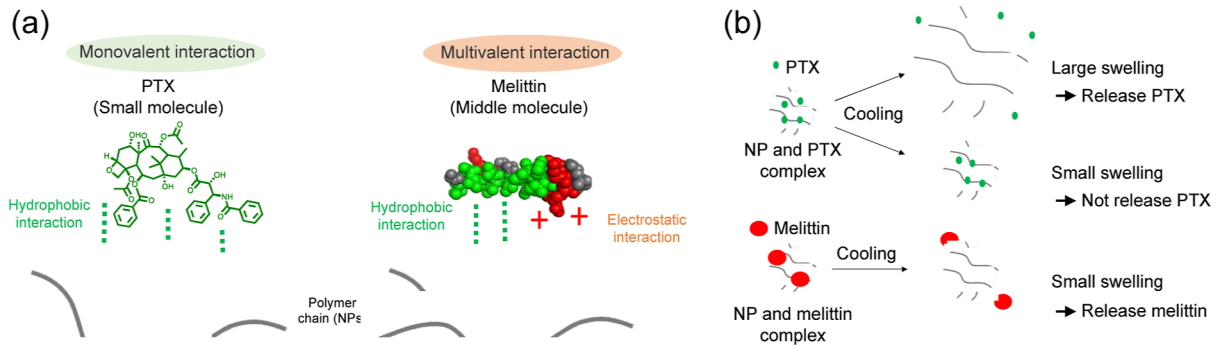

Figure 6. Schematic of NP−PTX and NP−melittin interactions and temperature-responsive release of target molecules from NPs: (a) NPs bind to PTX (a low-molecular-weight drug) via hydrophobic (monovalent) interactions and to melittin (a middle-molecular-weight peptide) via combined hydrophobic and electrostatic (multivalent) interactions. (b) Large and small swelling degrees elicit PTX and melittin release from TBAm NPs, respectively.

NPs, implying that T5-A5- and T10-A5-NPs lack sufficient hydrophobic monomer amounts for capturing melittin. Because T25-A5-NP (swelling ratio = 1.09) and T30-A5-NP (swelling ratio = 1.04) were not swelled by cooling from 37 to 25 °C, they were considered as temperature-unresponsive. In contrast, melittin incubated with T15-A5-NP (swelling ratio = 1.57) and T20-A5-NP (swelling ratio = 1.14) induced hemolysis at 25 °C but not at 37 °C, indicating that both NPs capture melittin at 37 °C and release it after cooling to 25 °C. We showed that a swelling ratio above 2 is required for PTX release from the NPs, although NPs with a smaller swelling ratio (1.14) released melittin in response to temperature. As shown in Figure 6a, NPs bind to PTX via monovalent (hydrophobic) interactions and to melittin via multivalent (electrostatic and hydrophobic) interactions. As PTX−NP interactions rely only on hydrophobic interactions, breakage of the PTX−NP bonds (i.e., PXT release) should require a substantial increase in hydrophilicity (Figure 6b). In contrast, the NPs bind to melittin via multivalent electrostatic and hydrophobic interactions. The T15-A5-NP and T20-A5-NP samples incorporated a minimum amount of the monomer for melittin capture. Therefore, a slight hydrophobicity-to-hydrophilicity change in the NPs should elicit a drastic change in the melittin affinity and release. This reasoning explains why T15-A5-NP and T20-A5-NP released melittin when swelled by a small amount. Among the PAA NPs, only P5-A5-NP inhibited hemolysis at 37 °C and induced only slight hemolysis at 25 °C. The other PAA NPs inhibited homolysis at both 37 and 25 °C. Although all PAA NPs swelled when cooled from 37 to 25 °C, only P5-A5-NP captured and released melittin in response to temperature. Unlike TBAm NPs, PAA NPs bind to melittin via $\pi-\pi$-stacking and hydrophobic interactions. The $\pi-\pi$ stacking interaction induced by the phenyl group of PAA is more stable than the sole hydrophobic interactions induced by the *tert*-butyl group of TBAm. TBAm NPs might capture PTX within the hydrophobic-rich environment created by *tert*-butyl groups.[31] In contrast, each phenyl group in the PAA NPs binds to one aromatic group (tryptophan) in melittin. These results imply that the release of captured molecules from NPs depends on the target and its mode of binding to the NPs.

CONCLUSIONS

pNIPAm-based NPs captured and released PTX, a hydrophobic small molecule (MW: 854), in response to temperature. To release its captured molecules (in the present case, PTX), the NPs must swell when cooled, although the NP swelling pattern depended on the structure of the hydrophobic monomer. TBAm percentage affected the onset temperature of the particle size increase but not the swelling ratio. In contrast, PAA percentage affected the swelling ratio but not the onset temperature of particle size increase. PTX was released from TBAm NPs only when the swelling ratio exceeded 2.0, but melittin (a midmolecular weight peptide, MW: 2847) was released at a swelling ratio of 1.1. Judging from these results, the amount of target molecules released from temperature-responsive NPs depends on both the structure and the percentage of the included hydrophobic monomer. Whereas the TBAm NPs released the captured target molecules (PTX and melittin) in large amounts, the PAA NPs released few of their captured target molecules. These results emphasize that optimizing the functional monomers of temperature-responsive NPs is essential for the effective catch and release of the target in a temperature-dependent manner. However, we did not incubate PTX-loaded NPs with the cell because of the NP stability problem. To improve NP stability, poly(ethylene glycol) modification should be a useful method. The present results are expected to provide useful information for designing synthetic polymers that catch and release their target molecule under a stimulus, such as temperature or pH.

MATERIALS AND METHODS

Materials. The following materials were obtained from commercial sources: *N*-isopropylacrylamide (NIPAm, ≥98.0% purity), acrylic acid (AAc, ≥99.0% purity), and *N*-phenylacrylamide (PAA, ≥98.0% purity) from Tokyo Chemical Industry Co., Ltd. (Tokyo, Japan); ammonium persulfate (APS, ≥98.0%, purity) and melittin (from honey bee, ≥85.0%) from Sigma-Aldrich, Inc. (St Louis, MO, USA); *N*,*N*′-methylenebis(acrylamide) (bis, ≥97.0%, purity), *N*-*tert*-butylacrylamide (TBAm, ≥95.0%, purity), sodium dodecyl sulfate (SDS, ≥95.0%, purity), PTX (≥98.0%, purity), and isoflurane (≥98.0% purity) from Wako Pure Chemical Industries, Ltd. (Osaka, Japan); *N*- Taxol, [^{3}H] from Moravek Biochemicals, Inc. (Brea, CA, USA); and Hionic Fluor from PerkinElmer Japan Co. Ltd. (Yokohama, Kanagawa, Japan). NIPAm was recrystallized from hexane (Wako Pure Chemical Industries, Ltd., 96.0%) before polymerization.

NP Synthesis. NIPAm, TBAm, AAc, PAA, bis, and SDS (4 mg) were dissolved in ultrapure water (20 mL). Prior to addition, TBAm and PAA were dissolved in ethanol (600 μL) and acetone (1000 μL), respectively. The total monomer concentration was 65 mM. The monomer solution was

https://doi.org/10.1021/acsomega.3c07226
ACS Omega 2024, 9, 1011−1019

degassed by nitrogen gas bubbling for 20 min. After the addition of APS aqueous solution (0.6 mg/mL), polymerization was carried out at 65 °C for 3 h under a nitrogen atmosphere. The polymerized solutions were purified by dialysis against excess pure water for more than 4 days.

Characterization of NPs. The particle size and polydispersity index (PDI) of the NPs were obtained from dynamic light scattering (DLS) measurements at 37 or 25 ± 0.1 °C. The DLS instrument was an Anton Paar LiteSizer 500 (Anton Paar GmbH, Graz, Austria). Each sample was dissolved in PBS (pH 7.4), and the swelling ratio was determined as

$$\text{Swelling ratio} = (\text{NP size at 25 °C})/(\text{NP size at 37 °C})$$

Hemolysis Assay. Bovine blood was washed with PBS, centrifuged (10,000*g*, 10 min, 4 °C) and washed an additional four times with PBS. The RBCs were resuspended in PBS (four times dilution), and the RBC solution was incubated with melittin (6×10^{-6} M) and/or NPs at 37 or 25 °C (total 200 μL) for 2 h after preincubating the melittin and NPs (n = 3). The culture was centrifuged (10,000*g* for 10 min at 4 °C), and the hemoglobin amount in the supernatant was calculated from the absorbance at 405 nm (Tecan Infinite M200 microplate reader). As a control (100% hemolysis), RBCs were incubated with 1% reduced Triton X-100.

Cell Culture. Colon26 NL-17 carcinoma cells (C26NL17) were cultured in Dulbecco's modified Eagle's medium, a high-glucose medium from Wako Pure Chemical Industries, supplemented with streptomycin (100 μg/mL) and penicillin (100 U/mL) from MP Biomedicals, Inc. (Solon, OH, USA) and 10% heat-inactivated fetal bovine serum from Thermo Fisher Scientific Inc. (Kanagawa, Japan). The culture was incubated at 37 °C in a 5% CO_2 atmosphere.

Binding of NPs to PTX. [^{3}H]-labeled PTX (100 nM) and NPs (1 mg/mL) were incubated at 37 °C for 30 min and ultracentrifuged (453,000*g*, 30 min, 37 °C) to precipitate the NPs. The radioactivity of free [^{3}H]-labeled PTX in the supernatant was measured by a liquid scintillation counter (LSC-7400, Hitachi Aloka Medical, Tokyo, Japan).

Cytotoxicity of PTX. C26NL17 cells were seeded in a 96-well plate at a density of 1.0×10^3 cells/well. The PTX (100 nM) and NPs (1 mg/mL) were incubated at 37 °C for 30 min and ultracentrifuged (453,000*g*, 30 min, 37 °C) to precipitate the NPs. After the supernatant was added, the cells were incubated at 37 °C for 24 h. The viable cells were determined by the WST-8 assay (n = 5) using cell counting kit-8 (Dojindo Laboratories, Kumamoto, Japan), which was added to each well as described in the technical manuals. After 1 h of incubation at 37 °C, the absorbance at 450 nm was measured using a Tecan Infinite M200 microscope reader.

Binding of NPs to PXT at 37 and 25 °C. Interactions between the NPs and PTX at 37 and 25 °C were monitored via ITC on a Malvern MicroCal iTC 200 instrument in the single injection mode. The NPs and PTX were prepared in 5 mM phosphate buffer (pH 7.4). Prior to ITC injection, all samples were degassed by centrifugation (3000*g*, 3 min). Using a syringe, 30 μL of PTX (350 nM) was titrated into the sample cell, filled with 210 μL of NP solution (3.5 mg/mL). The heat flow data (μcal/s) were collected at 1 s intervals until the signal returned to the baseline. Experiments were carried out at 37 or 25 °C with a stirring speed of 500 rpm.

■ ASSOCIATED CONTENT

Supporting Information

The Supporting Information is available free of charge at https://pubs.acs.org/doi/10.1021/acsomega.3c07226.

NMR data of NPs (PDF)

■ AUTHOR INFORMATION

Corresponding Author

Hiroyuki Koide − *Department of Medical Biochemistry, University of Shizuoka School of Pharmaceutical Sciences, Shizuoka, Shizuoka 422-8526, Japan*; orcid.org/0000-0003-1763-6593; Phone: +81-54-264-5701; Email: hkoide@u-shizuoka-ken.ac.jp; Fax: +81-54-264-5705

Authors

Kazuma Yamaguchi − *Department of Medical Biochemistry, University of Shizuoka School of Pharmaceutical Sciences, Shizuoka, Shizuoka 422-8526, Japan*

Keijiro Sato − *Department of Medical Biochemistry, University of Shizuoka School of Pharmaceutical Sciences, Shizuoka, Shizuoka 422-8526, Japan*

Maki Aoshima − *Department of Medical Biochemistry, University of Shizuoka School of Pharmaceutical Sciences, Shizuoka, Shizuoka 422-8526, Japan*

Shoko Kanata − *Department of Medical Biochemistry, University of Shizuoka School of Pharmaceutical Sciences, Shizuoka, Shizuoka 422-8526, Japan*

Sei Yonezawa − *Department of Medical Biochemistry, University of Shizuoka School of Pharmaceutical Sciences, Shizuoka, Shizuoka 422-8526, Japan*

Tomohiro Asai − *Department of Medical Biochemistry, University of Shizuoka School of Pharmaceutical Sciences, Shizuoka, Shizuoka 422-8526, Japan*

Complete contact information is available at: https://pubs.acs.org/10.1021/acsomega.3c07226

Author Contributions

All authors contributed to the contents of this manuscript and approved the final version of the manuscript.

Notes

The authors declare no competing financial interest.

■ ACKNOWLEDGMENTS

This work was supported by JSPS KAKENHI grant numbers 22H03957, 22H05051, and 19H04450.

■ ABBREVIATIONS

AAc, acrylic acid; APS, ammonium persulfate; bis, *N*,*N*′-methylenebis(acrylamide); CCK8, cell counting kit-8; C26 NL-17, colon26 NL-17 murine colon carcinoma; ITC, isothermal titration calorimetry; LCST, lower critical solution temperature; LMWD, low-molecular-weight drug; NIPAm, *N*-isopropylacrylamide; NP, polymer nanoparticle; PAA, *N*-phenylacrylamide; PDI, polydispersity index; PTX, paclitaxel; SDS, sodium dodecyl sulfate; TBAm, *N*-*tert*-butylacrylamide

■ REFERENCES

(1) (a) Koide, H.; Tsuchida, H.; Nakamoto, M.; Okishima, A.; Ariizumi, S.; Kiyokawa, C.; Asai, T.; Hoshino, Y.; Oku, N. Rational designing of an antidote nanoparticle decorated with abiotic polymer ligands for capturing and neutralizing target toxins. *J. Controlled*

https://doi.org/10.1021/acsomega.3c07226
ACS Omega 2024, 9, 1011−1019

Release **2017**, *268*, 335−342. (b) Hoshino, Y.; Taniguchi, S.; Takimoto, H.; Akashi, S.; Katakami, S.; Yonamine, Y.; Miura, Y. Homogeneous Oligomeric Ligands that Recognize and Neutralize a Target Peptide Prepared via Radical Polymerization. *Angew. Chem., Int. Ed. Engl.* **2020**, *59*, 679. (c) Sandanaraj, B. S.; Demont, R.; Aathimanikandan, S. V.; Savariar, E. N.; Thayumanavan, S. Selective sensing of metalloproteins from nonselective binding using a fluorogenic amphiphilic polymer. *J. Am. Chem. Soc.* **2006**, *128* (33), 10686−10687. (d) Tominey, A. F.; Liese, J.; Wei, S.; Kowski, K.; Schrader, T.; Kraft, A. RAFT polymers for protein recognition. *Beilstein J. Org. Chem.* **2010**, *6*, 66.

(2) (a) Dernedde, J.; Rausch, A.; Weinhart, M.; Enders, S.; Tauber, R.; Licha, K.; Schirner, M.; Zugel, U.; von Bonin, A.; Haag, R. Dendritic polyglycerol sulfates as multivalent inhibitors of inflammation. *Proc. Natl. Acad. Sci. U. S. A.* **2010**, *107* (46), 19679−19684. (b) Urner, L. H.; Mohammadifar, E.; Ludwig, K.; Shutin, D.; Fiorentino, F.; Liko, I.; Almeida, F. G.; Kutifa, D.; Haag, R.; Robinson, C. V. Anionic Dendritic Polyglycerol for Protein Purification and Delipidation. *ACS Appl. Polym. Mater.* **2021**, *3* (11), 5903−5911. (c) Chauhan, A. S.; Sridevi, S.; Chalasani, K. B.; Jain, A. K.; Jain, S. K.; Jain, N. K.; Diwan, P. V. Dendrimer-mediated transdermal delivery: enhanced bioavailability of indomethacin. *J. Controlled Release* **2003**, *90* (3), 335−343. (d) Chandrasekar, D.; Sistla, R.; Ahmad, F. J.; Khar, R. K.; Diwan, P. V. The development of folate-PAMAM dendrimer conjugates for targeted delivery of anti-arthritic drugs and their pharmacokinetics and biodistribution in arthritic rats. *Biomaterials* **2007**, *28* (3), 504−512.

(3) (a) Koide, H.; Fukuta, T.; Okishim, A.; Ariizumi, S.; Kiyokawa, C.; Tsuchida, H.; Nakamoto, M.; Yoshimatsu, K.; Ando, H.; Dewa, T.; et al. Engineering the Binding Kinetics of Synthetic Polymer Nanoparticles for siRNA Delivery. *Biomacromolecules* **2019**, *20* (10), 3648−3657. (b) Koide, H.; Yoshimatsu, K.; Hoshino, Y.; Lee, S. H.; Okajima, A.; Ariizumi, S.; Narita, Y.; Yonamine, Y.; Weisman, A. C.; Nishimura, Y.; et al. A polymer nanoparticle with engineered affinity for a vascular endothelial growth factor (VEGF165). *Nat. Chem.* **2017**, *9* (7), 715−722. (c) Koide, H.; Yoshimatsu, K.; Hoshino, Y.; Ariizumi, S.; Okishima, A.; Ide, T.; Egami, H.; Hamashima, Y.; Nishimura, Y.; Kanazawa, H.; et al. Sequestering and inhibiting a vascular endothelial growth factor in vivo by systemic administration of a synthetic polymer nanoparticle. *J. Controlled Release* **2019**, *295*, 13−20. (d) Mitchell, M. J.; Billingsley, M. M.; Haley, R. M.; Wechsler, M. E.; Peppas, N. A.; Langer, R. Engineering precision nanoparticles for drug delivery. *Nat. Rev. Drug Discovery* **2021**, *20* (2), 101−124.

(4) Xia, F.; Zuo, X.; Yang, R.; Xiao, Y.; Kang, D.; Vallee-Belisle, A.; Gong, X.; Yuen, J. D.; Hsu, B. B.; Heeger, A. J.; et al. Colorimetric detection of DNA, small molecules, proteins, and ions using unmodified gold nanoparticles and conjugated polyelectrolytes. *Proc. Natl. Acad. Sci. U.S.A.* **2010**, *107* (24), 10837−10841.

(5) Burg, T. P.; Godin, M.; Knudsen, S. M.; Shen, W.; Carlson, G.; Foster, J. S.; Babcock, K.; Manalis, S. R. Weighing of biomolecules, single cells and single nanoparticles in fluid. *Nature* **2007**, *446* (7139), 1066−1069.

(6) Stuart, M. A.; Huck, W. T.; Genzer, J.; Muller, M.; Ober, C.; Stamm, M.; Sukhorukov, G. B.; Szleifer, I.; Tsukruk, V. V.; Urban, M.; et al. Emerging applications of stimuli-responsive polymer materials. *Nat. Mater.* **2010**, *9* (2), 101−113.

(7) (a) MacKay, J. A.; Chen, M.; McDaniel, J. R.; Liu, W.; Simnick, A. J.; Chilkoti, A. Self-assembling chimeric polypeptide-doxorubicin conjugate nanoparticles that abolish tumours after a single injection. *Nat. Mater.* **2009**, *8* (12), 993−999. (b) Dhal, P. K.; Huval, C. C.; Holmes-Farley, S. R. Functional Polymers as Human Therapeutic Agents. *Ind. Eng. Chem. Res.* **2005**, *44* (23), 8593−8604. (c) Maitz, M. F. Applications of synthetic polymers in clinical medicine. *Biosurface and Biotribology* **2015**, *1* (3), 161−176. (d) Han, M.; Beon, J.; Lee, J. Y.; Oh, S. S. Systematic Combination of Oligonucleotides and Synthetic Polymers for Advanced Therapeutic Applications. *Macromol. Res.* **2021**, *29* (10), 665−680.

(8) Fleige, E.; Quadir, M. A.; Haag, R. Stimuli-responsive polymeric nanocarriers for the controlled transport of active compounds: concepts and applications. *Adv. Drug Delivery Rev.* **2012**, *64* (9), 866−884.

(9) Dai, S.; Ravi, P.; Tam, K. C. pH-Responsive polymers: synthesis, properties and applications. *Soft Matter* **2008**, *4* (3), 435−449.

(10) Jochum, F. D.; Theato, P. Temperature- and light-responsive smart polymer materials. *Chem. Soc. Rev.* **2013**, *42* (17), 7468−7483.

(11) Karimi, M.; Sahandi Zangabad, P.; Ghasemi, A.; Amiri, M.; Bahrami, M.; Malekzad, H.; Ghahramanzadeh Asl, H.; Mahdieh, Z.; Bozorgomid, M.; Ghasemi, A.; et al. Temperature-Responsive Smart Nanocarriers for Delivery Of Therapeutic Agents: Applications and Recent Advances. *ACS Appl. Mater. Interfaces* **2016**, *8* (33), 21107−21133.

(12) Manouras, T.; Vamvakaki, M. Field responsive materials: photo-electro-magnetic- and ultrasound-sensitive polymers. *Polym. Chem.* **2017**, *8* (1), 74−96.

(13) Shim, M. S.; Kwon, Y. J. Stimuli-responsive polymers and nanomaterials for gene delivery and imaging applications. *Adv. Drug Delivery Rev.* **2012**, *64* (11), 1046−1059.

(14) Alarcón, C. d. l. H.; Pennadam, S.; Alexander, C. Stimuli responsive polymers for biomedical applications. *Chem. Soc. Rev.* **2005**, *34* (3), 276−285.

(15) (a) Pelton, R. H.; Chibante, P. Preparation of aqueous latices with N-isopropylacrylamide. *Colloids Surf.* **1986**, *20* (3), 247−256. (b) Lutz, J. F.; Akdemir, O.; Hoth, A. Point by point comparison of two thermosensitive polymers exhibiting a similar LCST: is the age of poly(NIPAM) over? *J. Am. Chem. Soc.* **2006**, *128* (40), 13046−13047. (c) Matsumoto, K.; Sakikawa, N.; Miyata, T. Thermo-responsive gels that absorb moisture and ooze water. *Nat. Commun.* **2018**, *9*, 2315.

(16) Yu, Y.; Kieviet, B. D.; Liu, F.; Siretanu, I.; Kutnyánszky, E.; Vancso, G. J.; de Beer, S. Stretching of collapsed polymers causes an enhanced dissipative response of PNIPAM brushes near their LCST. *Soft Matter* **2015**, *11* (43), 8508−8516.

(17) Yoshimatsu, K.; Lesel, B. K.; Yonamine, Y.; Beierle, J. M.; Hoshino, Y.; Shea, K. J. Temperature-Responsive "Catch and Release" of Proteins by using Multifunctional Polymer-Based Nanoparticles. *Angew. Chem., Int. Ed.* **2012**, *51* (10), 2405−2408.

(18) Panja, S.; Dey, G.; Bharti, R.; Kumari, K.; Maiti, T. K.; Mandal, M.; Chattopadhyay, S. Tailor-Made Temperature-Sensitive Micelle for Targeted and On-Demand Release of Anticancer Drugs. *ACS Appl. Mater. Interfaces* **2016**, *8* (19), 12063−12074.

(19) Oya, T.; Enoki, T.; Grosberg, A. Y.; Masamune, S.; Sakiyama, T.; Takeoka, Y.; Tanaka, K.; Wang, G.; Yilmaz, Y.; Feld, M. S.; et al. Reversible molecular adsorption based on multiple-point interaction by shrinkable gels. *Science* **1999**, *286* (5444), 1543−1545.

(20) Chen, Y.; Wang, Z.; Harn, Y. W.; Pan, S.; Li, Z.; Lin, S.; Peng, J.; Zhang, G.; Lin, Z. Resolving Optical and Catalytic Activities in Thermoresponsive Nanoparticles by Permanent Ligation with Temperature-Sensitive Polymers. *Angew. Chem., Int. Ed. Engl.* **2019**, *58* (34), 11910−11917.

(21) (a) You, Y. Z.; Kalebaila, K. K.; Brock, S. L.; Oupicky, D. Temperature-controlled uptake and release in PNIPAM-modified porous silica nanoparticles. *Chem. Mater.* **2008**, *20* (10), 3354−3359. (b) Prawatborisut, M.; Oberlander, J.; Jiang, S.; Graf, R.; Avlasevich, Y.; Morsbach, S.; Crespy, D.; Mailander, V.; Landfester, K. Temperature-Responsive Nanoparticles Enable Specific Binding of Apolipoproteins from Human Plasma. *Small* **2022**, *18* (3), No. e2103138.

(22) (a) Bordat, A.; Boissenot, T.; Nicolas, J.; Tsapis, N. Thermoresponsive polymer nanocarriers for biomedical applications. *Adv. Drug Delivery Rev.* **2019**, *138*, 167−192. (b) Bolla, P. K.; Rodriguez, V. A.; Kalhapure, R. S.; Kolli, C. S.; Andrews, S.; Renukuntla, J. A review on pH and temperature responsive gels and other less explored drug delivery systems. *J. Drug Delivery Sci. Technol.* **2018**, *46*, 416−435.

(23) Zhang, J.; Qian, Z.; Gu, Y. In vivo anti-tumor efficacy of docetaxel-loaded thermally responsive nanohydrogel. *Nanotechnology* **2009**, *20* (32), 325102.

(24) Koide, H.; Saito, K.; Yoshimatsu, K.; Chou, B.; Hoshino, Y.; Yonezawa, S.; Oku, N.; Asai, T.; Shea, K. J. Cooling-induced, localized

https://doi.org/10.1021/acsomega.3c07226
ACS Omega 2024, 9, 1011−1019

release of cytotoxic peptides from engineered polymer nanoparticles in living mice for cancer therapy. *J. Controlled Release* **2023**, *355*, 745−759.
(25) Hoshino, Y.; Koide, H.; Furuya, K.; Haberaecker, W. W.; Lee, S. H.; Kodama, T.; Kanazawa, H.; Oku, N.; Shea, K. J. The rational design of a synthetic polymer nanoparticle that neutralizes a toxic peptide in vivo. *Proc. Natl. Acad. Sci. U.S.A.* **2012**, *109* (1), 33−38.
(26) Debord, J. D.; Lyon, L. A. Synthesis and characterization of pH-responsive copolymer microgels with tunable volume phase transition temperatures. *Langmuir* **2003**, *19* (18), 7662−7664.
(27) (a) Liu, H. Y.; Zhu, X. X. Lower critical solution temperatures of N-substituted acrylamide copolymers in aqueous solutions. *Polymer* **1999**, *40* (25), 6985−6990. (b) Miyazaki, H.; Kataoka, K. Preparation of polyacrylamide derivatives showing thermo-reversible coacervate formation and their potential application to two-phase separation processes. *Polymer* **1996**, *37* (4), 681−685.
(28) Nakayama, M.; Akimoto, J.; Okano, T. Polymeric micelles with stimuli-triggering systems for advanced cancer drug targeting. *J. Drug Targeting* **2014**, *22* (7), 584−599.
(29) Roth, P. J.; Collin, M.; Boyer, C. Advancing the boundary of insolubility of non-linear PEG-analogues in alcohols: UCST transitions in ethanol−water mixtures. *Soft Matter* **2013**, *9* (6), 1825−1834.
(30) Beierle, J. M.; Yoshimatsu, K.; Chou, B.; Mathews, M. A. A.; Lesel, B. K.; Shea, K. J. Polymer Nanoparticle Hydrogels with Autonomous Affinity Switching for the Protection of Proteins from Thermal Stress. *Angew. Chem., Int. Ed.* **2014**, *53* (35), 9275−9279.
(31) Okishima, A.; Koide, H.; Hoshino, Y.; Egami, H.; Hamashima, Y.; Oku, N.; Asai, T. Design of Synthetic Polymer Nanoparticles Specifically Capturing Indole, a Small Toxic Molecule. *Biomacromolecules* **2019**, *20* (4), 1644−1654.

https://doi.org/10.1021/acsomega.3c07226
ACS Omega 2024, 9, 1011−1019